Small-Angle X-Ray Scattering Analysis of Nanophase Titanium Dioxide, Poly[*N*-(4-sulfophenyl)aniline], and Their Composite

Nachagoni Narsimlu, Yen-Ding Kuo, Chun-Guey Wu

Department of Chemistry, National Central University, Chung-li, Taiwan 32054, Republic of China

Received 30 March 2002; accepted 9 September 2002

ABSTRACT: Small-angle X-ray scattering and spectroscopic (infrared and ultraviolet–visible) techniques were used to investigate the interactions between titanium dioxide (TiO_2) and the semiconductor polymer poly[*N*-(4-sulfophenyl)aniline] (PSA) in a poly[*N*-(4-sulfophenyl)aniline]/TiO_2 composite (TPSA). The radius of gyration of the cross section, the radius and length of the rodlike particle, the persistence length, the surface fractal dimension, and the PSA layer thickness on TiO_2 in aqueous solutions and in powder form were calculated. The results indicated that the aggregation of TiO_2 particles on drying was reduced by the formation of the composite with the semiconductor polymer. Only the particle length of the TPSA particle (which had a rodlike shape) increased on drying, probably because of increasing void sizes and the formation of aggregation. The persistence length of the TPSA particles decreased with respect to its individual components. The PSA layer thickness on TiO_2 was about 3.6 nm and decreased (to 2.6 nm) on dehydration because of the expulsions of water molecules from the TiO_2/PSA composite. © 2003 Wiley Periodicals, Inc. J Appl Polym Sci 88: 3183–3187, 2003

Key words: SAXS; water-soluble polymers; nanocomposites

INTRODUCTION

The sophisticated use of different semiconductors and semiconductor/polymer-based composites may hold the key role to developing new structures and devices in many advanced technological industries.[1–3] Among these, the titanium dioxide (TiO_2) oxide semiconductor and its composites have a number of industrial applications, such as light-emitting diodes, photodetectors, photodiodes, photoconductors, and photovoltaic cells. TiO_2 can also be used as an eliminator of organic pollutants in aqueous solutions or in air as a self-cleaning smart material.[4–6] TiO_2 has the highest photocatalytic activity among oxide semiconductors with three crystal phases.[6,7] However, a crucial practical difficulty with this TiO_2 semiconductor is its wide bandgap (3.2 eV, 387 nm), which lies outside of the most intense solar spectrum (2.48 eV, 500 nm).[8] Scientists are trying to reduce its bandgap by adding some other metals to it, but no significant success has been reported because of experimental difficulties.[6,7] Now, some researchers are concentrating on the synthesis and characterization of TiO_2 semiconductor/polymer-based composite materials to enhance the photophysical properties by reducing the bandgap of TiO_2.[9–11]

However, conjugated polymers have a high absorption coefficient in the visible part of the solar spectrum, and they easily transfer photogenerated charge carriers to the TiO_2 electron acceptor with a unit of quantum efficiency.[12–15] Moreover, most of the optical and transport properties, such as the photoconductivity, microwave-frequency dielectric constant, direct-current electrical conductivity, and thermoelectric power, of these composites depend on the polymer chain alignment with the inorganic semiconductor.[16] Therefore, the structure–property relationship of these composites has been a field extensively studied. Different experimental techniques are available for determining the macromolecular arrangement of these composite materials and their individual components. These include transmission electron microscopy (TEM), scanning electron microscopy, and X-ray and neutron diffraction. Among these, small-angle X-ray scattering (SAXS) is a useful and nondestructive technique for estimating the considerable information for macromolecular parameters in dilute solutions, powders, and thin films.[17,18] In this study, we used spectroscopic techniques to confirm composite formation and SAXS to evaluate invariants of anisometric particles of the poly[*N*-(4-sulfophenyl)aniline]/TiO_2 composite (TPSA) both in solution and as a solid. The invariants evaluated in these systems include the radius of gyration of the cross section (R_c), the length of

Correspondence to: C.-G. Wu (t610002@cc.ncu.edu.tw).

Contract grant sponsor: National Science Council of Taiwan.

Journal of Applied Polymer Science, Vol. 88, 3183–3187 (2003)
© 2003 Wiley Periodicals, Inc.

the rodlike particles (L), the persistence length (a^*), and the thickness (E) of the poly[*N*-(4-sulfophenyl) aniline] (PSA) polymer layer on TiO_2. For comparison, the same experiments were done on the individual components TiO_2 and PSA.

EXPERIMENTAL

Materials

Ti(O-*i*-Pr)$_4$, isopropanol, *N*-(4-sulfophenyl)aniline, $(NH_4)_2S_2O_8$, and aqueous HCl were purchased from commercial resources and used as received.

Preparation of the TiO_2 sol solution

Ti(O-*i*-Pr)$_4$ (2 mL) was dissolved in 20 mL of isopropanol and cooled in an ice bath. To it, a 0.7*M*, 360-mL aqueous HNO_3 solution (cooled at 4°C) was added slowly (8 mL/min) under violent stirring. The mixture was stirred at 4°C for 4 h. The solution became transparent, and a TiO_2 sol, with a diameter at about 10 nm, was formed. The sol solution was stable at 4°C for 2 weeks.

Synthesis of the water-soluble polyaniline PSA

N-(4-Sulfophenyl)aniline (1 g) was dissolved in 30 mL of 1.2*M* aqueous HCl. To it, 8.8 mmol of an aqueous $(NH_4)_2S_2O_8$ solution (in 30 mL of 1.2*M* aqueous HCl) was added. The mixture was stirred at room temperature for 20 h. The dark green precipitate was isolated with centrifugation, washed with dilute aqueous HCl several times, and dried under the ambient atmosphere.

Preparation of TPSA

PSA [0.01 g, 4.1 $\times 10^{-5}$ mol (of monomer)] was dissolved in 3.3 mL of water, and 20 mL of the TiO_2 (3.5 $\times 10^{-4}$ mol) sol solution was added to it. The mixture was stirred at room temperature for 10 min and then stored in a vial before the SAXS analysis. The powder was obtained by the slow evaporation of the solvent with an evaporator.

Physicochemical studies

The infrared (IR) spectra were obtained with a Bio-Rad model FT-155 Fourier transform infrared spectrophotometer. The room-temperature optical absorption spectrum of these materials was recorded with a Varian model Cary 5E spectrometer in the 190–1000-nm wavelength region. The SAXS experiments were performed at the X-ray scattering laboratory of the Department of Engineering and System Science at Tsing Hua University. The X-ray source was an 18-kW rotating-anode X-ray generator equipped with a copper target. The incident Cu Kα X-ray (λ = 0.15418 nm) beam was monochromated by graphite crystal and collimated subsequently by three pinhole slits. A two-dimensional area proportional counter was employed to detect the scattered X-rays. The scattering intensities were recorded by 250 pixels, and the data were stored in a personal computer. The scattering vector ($\mathbf{Q} = 4\Pi \sin \theta/\lambda$) was determined from 0.04 to 1.44 nm^{-1}. The counting time lasted for more than 2 h so that good counting statistics could be obtained. An empty sample cell was used to obtain a blank scattering; consequently, background subtraction was carried out on all data. No correction was made for fluctuations in the beam intensity.

RESULTS AND DISCUSSION

The IR spectra of TPSA and its individual components exhibit well-known absorption bands. No unusual bands are observed in the composite formation because IR inactivates TiO_2. The absorption threshold wavelength of TPSA is similar to that of TiO_2 at room temperature, and this indicates that there is no interband charge transfer between PSA and TiO_2. Nevertheless, after the refluxing, the onset wavelength (optical bandgap) of the composite increases from 329 to 400 nm. This is because the structure of PSA changes after the refluxing. The interband change transfer between TiO_2 and heat-treated PSA becomes possible. A detailed study of the interactions between TiO_2 and PSA under various reaction conditions will be reported elsewhere.[15]

TiO_2 in an aqueous solution can be considered an amorphous material with aggregates containing TiO_2 nanograins because the X-ray absorption near-edge structure shows that titanium in twofold oxygen geometry is postulated to be amorphous, whereas sixfold and fivefold oxygen geometries are considered octahedral and square pyramidal crystalline geometries, respectively.[11] Under these conditions, SAXS by TiO_2 particles (as well as PSA and their composites) takes place because of the difference in the electron densities of the solvent and solute. With the Guinier approximation, the size of the particles can readily be determined:

$$I(\mathbf{Q}) = L^*II/\mathbf{Q}^*I_c(\mathbf{Q}),\ I_c(\mathbf{Q}) = I_c(0)\exp(-\mathbf{Q}^2R_c^2/2) \quad (1)$$

where 2θ is the scattering angle and λ is the wavelength of the Cu Kα X-ray (0.15418 nm). The average particle radius (R) is estimated from R_c in the Guinier formula from the slopes of linear fittings of curves of $\log[\mathbf{Q}I(\mathbf{Q})]$ versus $\mathbf{Q}^2$ (Fig. 1), with $R = \sqrt{2}R_c$ for

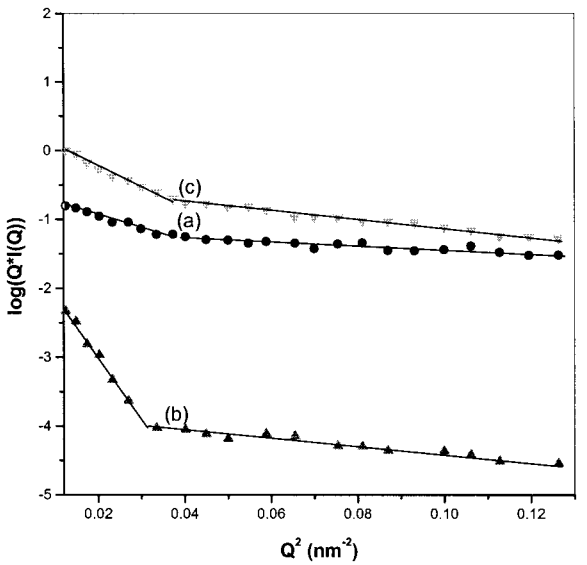

Figure 1 Guinier plot for (a) TiO_2, (b) PSA, and (c) TPSA particles in aqueous solutions.

rodlike particles.[19] L of these rodlike particles can be estimated as follows:

$$L = \pi I(0)/lim_{\mathbf{Q}\to 0}[\mathbf{Q}I(\mathbf{Q})] \quad (2)$$

where $I(0)$ is the scattered intensity extrapolated to the zero scattering vector.[19] Figures 2(c) and 3(c) represent the extrapolated $I(0)$ and $\lim_{\mathbf{Q}\to 0}[\mathbf{Q}I(\mathbf{Q})]$ values for TPSA. Similarly, the same approximation is applied for the amorphous PSA and TiO_2 rodlike particles [Figs. 2(a,b) and 3(a,b)]. The radii and lengths of PSA, TiO_2, and their composite in solution and in powder form are tabulated in Table I. The TEM micrographs of TiO_2 and TPSA clearly reveal that the particles of TiO_2

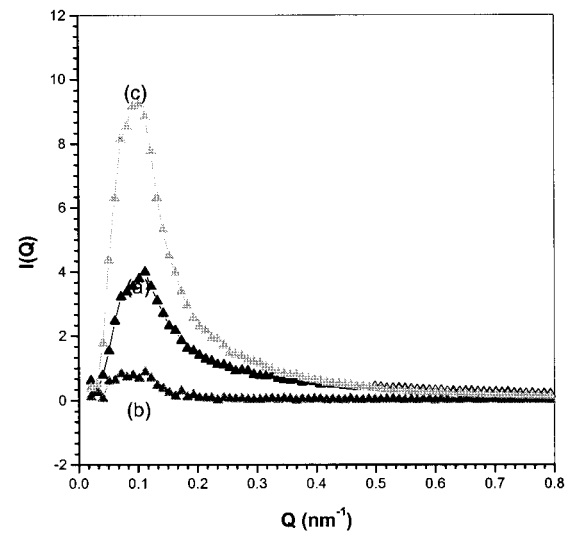

Figure 2 Linear plot of (a) TiO_2, (b) PSA, and (c) TPSA particles in aqueous solutions [$I(\mathbf{Q})$ vs $\mathbf{Q}$] extrapolated to a zero scattering vector.

TABLE I
Physical Parameters of TiO_2, PSA, and TPSA in Aqueous Solutions (1–3) and in Powder Form (4–6).

	System	R_c (nm)	R (nm)	L (nm)
1	TiO_2	6.3	8.9	502.4
2	PSA	11.5	16.3	266.9
3	TPSA[a]	10.0	14.1	1452.0
4	TiO_2	13.5	19.1	2433.5
5	PSA	12.0	16.90	1081.6
6	TPSA[a]	11.80	16.70	7379.5

[a] The molar ratio of TiO_2 to PSA was 10:1 for the TPSA composite.

in the solution are rodlike, with lengths of 450 and 500 nm, respectively.[15] The particle size of TiO_2 obtained from SAXS data is quite consistent with that from the TEM data. Nevertheless, there is a difference between the particle sizes estimated by SAXS and TEM micrographs for the TiO_2/polymer composite. This may be assigned to the inhomogeneous particle size of the materials (some unreacted PSA is also present in the solution). In TEM, only a limited number particles will be focused under the microscope, but in SAXS, an average of all particles size is calculated. Another possibility for the difference in the particle size obtained from the two differently measured systems may be that there is an aggregation of TPSA particles in solution. The aggregation is broken by ultrasonication during TEM sample preparation. Nevertheless, Table I shows that the lengths of all the particles studied increase when the samples are dried. This may be due to the aggregation of particles or the expansion of voids at the time of drying, as reported by Crawshaw and Camerson.[20–23] Table I also shows that the particle radius of TiO_2 increases two times, but the radii of PSA and TPSA do not change significantly on drying. The results imply that the aggregation of TiO_2 is reduced by the formation of the composite with the conjugated polymer.

SAXS is also a good technique for determining a^* of a particle in a solution. Originally, it was defined by Kratky and Porod as an average length that a particle can persist in a particular direction.[24,25] As such, it may be taken as a measure of the stiffness of the chains. It can be calculated with a Kratky plot of $\mathbf{Q}^2I(\mathbf{Q})$ versus $\mathbf{Q}$. The transition point $\mathbf{Q}^*$, from the asymptotic values for the Gaussian coil to the asymptotic values for the rod, can be determined by the condition of intersection.[19,21] a^* can be calculated with eq. (3), in which K is a constant (set at 2.74 in this work), λ is the wavelength of the X-ray, $\mathbf{Q}^*$ is equal to $4\pi \sin\theta^*/\lambda$, and $\sin\theta^*$ is approximately θ^* when θ^* is very small:

$$a^* = (1/2.74)(2\pi/\mathbf{Q}^*), \text{ i.e. } a^* = 2.29/\mathbf{Q}^* \quad (3)$$

By estimating the $\mathbf{Q}^*$ value (Fig. 4) from the plot, we can find a^*. The calculated values for TiO_2, PSA, and

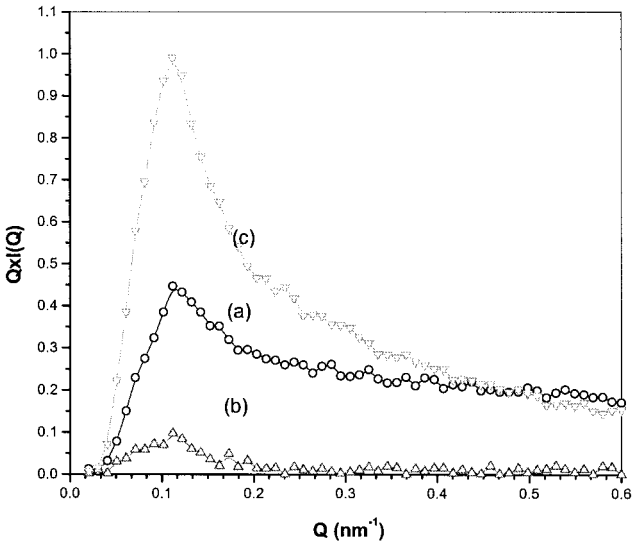

Figure 3 Extrapolation of a plot [$\mathbf{Q}I(\mathbf{Q})$ vs $\mathbf{Q}$] for the lower scattering vector of (a) TiO_2, (b) PSA, and (c) TPSA particles in aqueous solutions.

their composite TPSA in aqueous solutions are listed in Table II. Similarly, the surface fractal dimension (D_s) of these particles can be calculated with the help of SAXS data with eq. (4) and Figure 5:

$$\ln I(\mathbf{Q}) = \ln I_0 + (-\alpha)^* \ln \mathbf{Q} \quad (4)$$

where α and I_0 are constant and D_s is equal to $6 - \alpha$. If D_s is equal to 2, the surface is considered to be very smooth, whereas increasing the roughness of the surface causes an increase in D_s.[22] The calculated D_s values (see Table II) show that D_s of the composite (TPSA) is less than that of TiO_2 [the scattering intensity of PSA is very low; the D_s value obtained from its ln $I(\mathbf{Q})$–ln($\mathbf{Q}$) plot has some uncertainty]. The result indicates that the TPSA surface is smoother than that of TiO_2. Therefore, the mass and area of contact between the solvent and particles are lower for TPSA than for TiO_2. This leads to a reduction in a^* of TPSA.

TABLE II
a^* and D_s Values of TiO_2 PSA, and TPSA in Aqueous Solutions

	System	a^* (nm)	D_s
1	TiO_2	39.3	4.5
2	PSA	43.2	3.9
3	TPSA[a]	32.7	3.9

[a] The molar ratio of TiO_2 to PSA was 10:1 for the TPSA composite.

We also calculated E of the PSA layer on TiO_2 in TPSA in both solution and solid forms. Originally, this method was reported by Vonk, and it was later modified by Ruland.[19] According to Vonk, $\mathbf{Q}$ can be calculated as follows:

$$\mathbf{Q} = 2\pi^2 [\psi(1-\psi) - E/6 \{\pi\psi(1-\psi) \div \mathbf{Q} \lim_{\mathbf{Q}\to\infty} (\mathbf{Q}^4 I(\mathbf{Q}))\}] (\rho_c - \rho_a)^2 V \quad (5)$$

The modified Ruland model of this equation for the scattering intensity is $I(\mathbf{Q})$:

$$I(\mathbf{Q}) \approx B/\mathbf{Q}4^*(1 - 2E^2\mathbf{Q}^2/3)$$
$$I(\mathbf{Q})^* \mathbf{Q}4 = B(1 - 2E^2\mathbf{Q}^2/3) \quad (6)$$

where B is a constant. Equation (6) is valid for the asymptote at large scattering vectors, and an analysis of the relation between $\mathbf{Q}^4I(\mathbf{Q})$ and $\mathbf{Q}^2$ allows the estimation of E. With the help of the slope of the plot of $\mathbf{Q}^4I(\mathbf{Q})$ versus $\mathbf{Q}^2$, the E values of TPSA in solution and powder forms are calculated to be 3.52 and 2.68

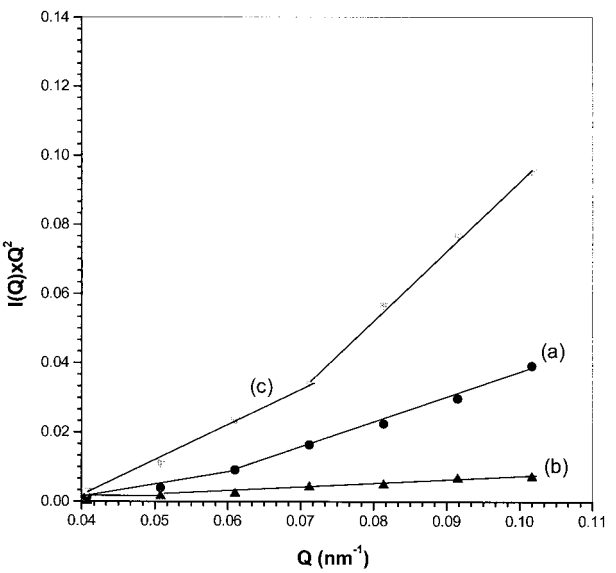

Figure 4 Plot of $I(\mathbf{Q}) \times \mathbf{Q}^2$ versus $\mathbf{Q}$ for (a) TiO_2, (b) PSA, and (c) TPSA particles in aqueous solutions.

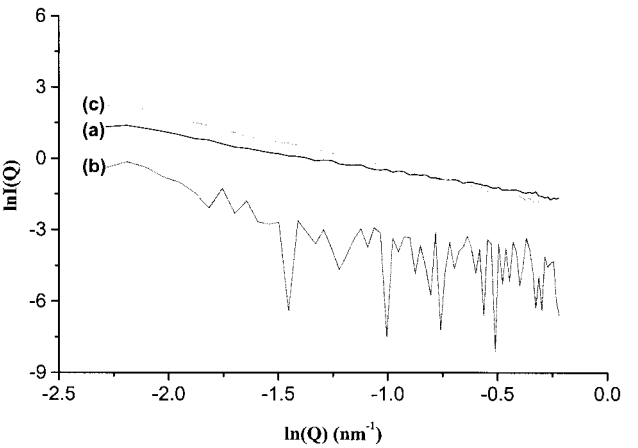

Figure 5 Plot of ln $I(\mathbf{Q})$ versus ln $\mathbf{Q}$ for (a) TiO_2, (b) PSA, and (c) TPSA particles in aqueous solutions.

nm, respectively. These values reveal that there is a reduction in the layer thickness on drying. This may be due to the water, which is present between the TiO_2 and PSA layers, being driven out after drying, as also observed by Pikus and others.[17,26–28]

CONCLUSIONS

This study reveals the possibility of investigating the interactions between the nanocrystalline TiO_2 and the conjugated polymer PSA in TPSA with the SAXS technique. Particles of TPSA and its individual components (TiO_2 and PSA) show a rodlike morphology. The radius of TPSA does not increase as much as that of TiO_2 on drying, and this indicates that the aggregation of TiO_2 is reduced by the formation of the composite. The lengths of all the particles increase on drying because of aggregation and void expansion. The a^* value of the composite is less than those of TiO_2 and PSA, and this suggests that the weight of the composite particles is heavier and that the conjugated polymer on the surface of TiO_2 makes the composite less stiff than its individual component TiO_2. SAXS is a good nondestructive experimental technique for evaluating different invariants of a semiconductor/polymer-based composite material and its components.

References

1. Heeger, A. J. Angew Chem Int Ed 2001, 40, 2591.
2. Yeh, Y.-R.; Hsia, H.-T.; Wu, C.-G. Synth Met 2001, 121, 1651.
3. Salafsky, J. S.; Lubberhuizen, W. H.; Schropp, R. E. I. Chem Phys Lett 1998, 290, 297.
4. Kominami, H.; Kohno, M.; Kera, Y. J Mater Chem 2000, 10, 1151.
5. Rajeshwar, K.; de Tacconi, N. R.; Chentamarkashan, C. R. Chem Mater 2001, 13, 2765.
6. Song, K. Y.; Park, M. K.; Kwon, Y. T.; Lee, H. W.; Chung, W. J.; Lee, W. I. Chem Mater 2001, 13, 2349.
7. Eibl, S.; Gates, B. C.; Knozinger, H. Langmuir 2001, 17, 107.
8. Asahi, R.; Morikawa, T.; Ohwaki, T.; Aoki, K.; Taga, Y. Science 2001, 293, 269.
9. Savenike, T. J.; Warman, J. M.; Goosens, A. Chem Phys Lett 1998, 287, 148.
10. Provenzano, P. L.; Gopi, R. J.; Sweet, J. R.; White, W. B. J Lumin 2001, 92, 297.
11. Leite, E. R.; Carreno, N. L. V.; Santos, L. P. S.; Rangel, J. H.; Soledade, L. E. B.; Longo, E.; Campos, C. E. M.; Lanciotti, F., Jr.; Pizani, P. S.; Varela, J. A. Appl Phys A 2001, 73, 567.
12. Wang, D.; Wang, J.; Guillermo, D. M.; Bazan, C.; Heeger, A. J. Langmuir 2001, 17, 1262.
13. Lonergan, M. C. Science 1997, 278, 2103.
14. Salasky, J. S.; Kerp, H.; Schroop, R. E. I. Synth Met 1999, 102, 1256.
15. Wu, C.-G.; Ting, K. Y.; Narsimlu, N. Submitted.
16. Joo, J.; Long, S. M.; Pouget, J. P.; Oh, J. E.; MacDiarmid, A. G.; Epstein, A. J. Phys Rev B 1998, 57, 9567.
17. Crawshaw, J.; Camesron, R. E. Polymer 2000, 41, 4691.
18. Timothy, J.; Stivala, T. S. S. Polymer 1996, 37, 715.
19. Feigen, L. A.; Svergun, D. I. Structure Analysis by Small-Angle X-Ray and Neutron Scattering; Plenum: New York, 1987.
20. Crawshaw, J.; Camesron, R. E. Polymer 2000, 41, 4691.
21. Timothy, J.; Stivala, T. S. S. Polymer 1996, 37, 715.
22. Li, X. K.; Liu, L.; Li, Z. H.; Wu, D.; Shen, S. D. Carbon 2000, 38, 623.
23. Sastry, P. U.; Sen, D.; Mazumder, M.; Chandrasekaran, K. S. Solid State Commun 2000, 114, 329.
24. Kratky, O.; Glatter, O. Small Angle X-ray Scattering; Academic Press: New York, 1982.
25. Porod, G. J Polym Sci 1953, 10, 157.
26. Vickers, M. E.; Briggs, N. P.; Ibbet, R. N.; Payne, J. J.; Smith, S. B. Polymer 2001, 42, 8241.
27. Pikus, S.; Dawidowicz, A. L.; Kobylas, E.; Wianowska, D. Mater Chem Phys 2001, 70, 181.
28. Pikus, S.; Dawidowicz, A. L.; Kobylas, E.; Wianowska, D. Appl Surf Sci 2000, 156, 189.